Phase coexistence in films composed of DLPC and DPPC: A comparison between different model membrane systems

CrossMark

Agustín Mangiarotti, Benjamín Caruso, Natalia Wilke *

Centro de Investigaciones en Química Biológica de Córdoba (CIQUIBIC), Departamento de Química Biológica, Facultad de Ciencias Químicas, Universidad Nacional de Córdoba, Córdoba, Argentina

ABSTRACT

For the biophysical study of membranes, a variety of model systems have been used to measure the different parameters and to extract general principles concerning processes that may occur in cellular membranes. However, there are very few reports in which the results obtained with the different models have been compared. In this investigation, we quantitatively compared the phase coexistence in Langmuir monolayers, freestanding bilayers and supported films composed of a lipid mixture of DLPC and DPPC. Two-phase segregation was observed in most of the systems for a wide range of lipid proportions using fluorescence microscopy. The lipid composition of the coexisting phases was determined and the distribution coefficient of the fluorescent probe in each phase was quantified, in order to explore their thermodynamic properties. The comparison between systems was carried out at 30 mN/m, since it is accepted that at this or higher lateral pressures, the mean molecular area in bilayers is equivalent to that observed in monolayers. Our study showed that while Langmuir monolayers and giant unilamellar vesicles had a similar phase behavior, supported films showed a different composition of the phases with the distribution coefficient of the fluorescent probe being close to unity. Our results suggest that, in supported membranes, the presence of the rigid substrate may have led to a stiffening of the liquid-expanded phase due to a loss in the degrees of freedom of the lipids as a consequence of the proximity of the solid material.

© 2014 Elsevier B.V. All rights reserved.

1. Introduction

The biophysical properties of biomembranes have been investigated using various models, such as Langmuir films, free-standing bilayers and supported films. Moreover, lipid membranes of a variety of compositions, and even natural membranes, have been studied as well as the effect of the presence of proteins.

The use of different model membranes permits a wide variety of experimental approaches: in Langmuir monolayers (LMs), the molecular density can be varied while the surface tension and surface potential are registered, and the membrane can be simultaneously observed with Brewster angle microscopy (BAM) or fluorescence microscopy (FM). Using FM, giant unilamellar vesicles (GUVs) can also be investigated along with the deformations out of the plane of the membrane. In planar free-standing bilayers, particle tracking and membrane permeability may be determined in a simpler way than in GUVs, but the film stability is lower. The supported lipid bilayers are usually deposited on a hydrophilic solid surface (glass, mica, or silicon) using several techniques of preparation such as spin-coating [1], vesicle rupture [2], solution

spreading [3] or film transfer from an LM through the Langmuir–Blodgett or the Langmuir–Schaefer technique [4]. The main advantage of supported lipid bilayers over water/air interface monolayers or vesicular systems is that they may be characterized by using a number of advanced techniques, such as atomic force microscopy [4], X-ray diffraction [5], neutron reflectivity [6], and quartz crystal microbalance [7].

Each of these model systems has certain advantages and disadvantages, depending on the situation in which one is more suitable to use. Related to this, cell membranes in biological systems cannot necessarily be considered similar to free-standing bilayers, since they are often interacting with (and supported by) cytoskeletal proteins, neighboring membrane stacks and extracellular matrices, with these interactions affecting the native lipid phase behavior. Therefore, in order to fully exploit the existing membrane model systems to retrieve biologically relevant information, it is important to have an as clear as possible understanding about the influence of preparation conditions on the lipid film.

In this work, the composition and properties of the coexisting phases were compared in different model membranes composed of a binary lipid mixture of 1,2-dilauroyl-sn-glycero-3-phosphocholine (DLPC) and 1,2-dipalmitoyl-sn-glycero-3-phosphocholine (DPPC). The phase diagram of LMs of this mixture was constructed, and monolayers were transferred to a glass support or hydrophobic hollow grids at 30 mN/m. In addition, supported bilayers were prepared from the rupture of

* Corresponding author at: CIQUIBIC, Dpto. de Química Biológica, Facultad de Ciencias Químicas, Universidad Nacional de Córdoba, Haya de la Torre y Medina Allende, Ciudad Universitaria, X5000HUA Córdoba, Argentina. Tel./fax: +54 351 5353855.

E-mail address: wilke@mail.fcq.unc.edu.ar (N. Wilke).

small unillamellar vesicles (SUVs), with GUVs also being studied as a free-standing model.

A comparison between supported films and LMs was carried out at 30 mN/m, since it has been postulated that between 30 and 35 mN/m, the mean molecular area in bilayers is equivalent to that observed in monolayers [8,9], although thermal fluctuations may lead to variations in the lateral pressure [10].

Our results showed that while the phase diagrams of LMs and GUVs were quite similar, the phase boundaries of the supported systems were shifted to higher DPPC proportions. Short-distance specific interactions between the support and the lipid membrane were discarded, but the proximity to the glass resulted in a loss of entropy of the films. Furthermore, an analysis of the fluorescent probe distribution coefficient between the phases in each model showed that as the degrees of freedom decreased from one system to the other, the properties of the two phases became more similar. These results suggest that the liquid-expanded phase was stiffer in the supported systems.

We conclude that even when working with a simple phospholipid mixture, the properties of the phases change between the different model membranes, thus it is important to determine the validity of the measured parameters extracted from each model in order to be able to generalize and extend the obtained results to more complex systems such as biological membranes.

2. Materials and methods

2.1. Materials

1,2-Dipalmitoyl-sn-glycero-3-phosphocholine (DPPC), 1,2-dilauroyl-sn-glycero-3-phosphocholine (DLPC) and the lipophilic fluorescent probe L-α-phosphatidylethanolamine-N-(lissaminerhodamine B sulfonyl) ammonium salt (PE-Rho) were purchased from Avanti Polar Lipids (Alabaster, AL, USA). Squalene was obtained from Merck, and octadecylthiol (ODT) and bovine serum albumin (BSA) from Sigma-Aldrich Co. (USA).

Lipid mixtures were prepared in Cl_3CH/CH_3OH 2:1 v/v to obtain a solution of 1 nmol/μL total concentration with all the solvents and chemicals used being of the highest commercial purity available. The subphase in all the experiments was deionized water with a resistivity of 18 MΩ cm, obtained from a Milli-Q Gradient System (Millipore, Bedfore, MA).

The glass coverslips (12 mm diameter) used for the supported membranes were purchased from Marienfeld GmbH & Co. Kg (Germany), and the transmission electron microscopy (TEM) grids used for assembling the planar freestanding lipid membranes were obtained from SPI Supplies (West Chester, USA).

2.2. Surface pressure-area measurements

Compression isotherms were carried out for different proportions of the lipid mixture at 21 ± 1 °C, with the desired composition being prepared and spread onto a KSV minitrough (KSV Instruments, Ltd. Helsinki, Finland) filled with deionized water up to a mean molecular area higher than the lift-off area. The surface pressure (π) was determined with a platinum plate using the Wilhelmy method, and the total film area was continuously measured and recorded while compressing at rates between 1 and 5 Å^2 molecules^{-1} min^{-1}. Each compression isotherm was repeated at least three times, with the difference in surface pressure and mean molecular area (MMA) between isotherms of independent experiments being less than 0.5 mNm^{-1} and 2 Å^2, respectively.

2.3. Preparation of supported lipid membranes

2.3.1. Transferred from monolayers (SMLs and SBLs)

The glass coverslips were treated with piranha solution (H_2SO_4: H_2O_2 3:1 v/v) at 90 °C for 60 min and rinsed with Milli-Q water. In this way, any organic matter remaining was removed and the surface became highly hydrophilic. Supported monolayers (SMLs) and bilayers (SBLs) were then formed by transferring the Langmuir monolayers (LMs) onto these coverglasses. To generate SMLs, the desired composition of the DPPC:DLPC mixture containing 1% PE-Rho was first compressed up to 30 mN/m. The monolayer was allowed to stabilize (~100 s), before being transferred by the Langmuir–Blodgett (LB) technique to the previously submerged hydrophilic substrate (oriented perpendicular to the trough), while maintaining the surface pressure constant. The supported monolayer remained in air for the duration of the experiments.

Two kinds of SBLs were studied: ^{d}SBLs, in which the mixed film with the fluorescent probe was in the distal leaflet (located more distant from the glass), and ^{p}SBLs with the film under study being in the proximal leaflet.

All ^{d}SBLs were generated by transferring a monolayer of DPPC using the LB technique as explained above, followed by the transference of the desired lipid mixture with the fluorescent probe using the Langmuir–Schaefer technique, i.e. the hydrophobic substrate generated by the LB transfer was submerged with an orientation parallel to the water surface. For the ^{p}SBLs, the mixed monolayer containing PE-Rho was first transferred by the LB method, and then a DPPC monolayer was transferred using the Langmuir–Schaefer technique. After the second transfer, a supported bilayer was generated, which was maintained under water. For all these systems, the transfer rate was 5 mm/min and the pressure was kept constant at 30 mN/m.

2.3.2. Formed from the rupture of vesicles (SVRs)

Small unilamellar vesicles (SUVs) of different phospholipid proportions were generated using the tip sonication method described by Lin et al. [2]. Briefly, the lipid mixtures in $Cl_3CH:CH_3OH$ were dried in a clean vial under a stream of N_2, and the lipids were resuspended in Milli-Q water to a final concentration of 0.5 mg/mL. The suspension was then incubated in a 50 °C water bath for 5 min with vortexing periods of 30 s. Finally, the suspension was sonicated using a tip sonicator Ultrasonic Homogenizer 4710 Series (Cole-Parmer Instruments Co., Chicago, Illinois, USA) and vesicles of 15–30 nm diameter were obtained. Size determinations were made by dynamic light scattering, using a submicron particle sizer NICOMP 380 (PSS.NICOMP, Santa Bárbara, California, USA).

A 100 μL droplet of the SUV suspension was placed on a hydrophilic glass coverslip (previously cleaned with piranha solution as explained in Section 2.3.1) and left for incubation for 15 min. Next, the coverslip was rinsed with Milli-Q water to remove the unadsorbed vesicles, and in this way, supported lipid bilayers were generated by the vesicle rupture onto the coverglass (SVRs).

2.4. Freestanding lipid bilayers

2.4.1. Planar lipid bilayers (PLBs)

Planar lipid bilayers (PLBs) were formed using gold-coated TEM grids as substrates, as reported by Harland et al. [11], by employing 1 mm-diameter gold grids with 200 hexagonal holes of 100 μm diameter. These grids were incubated with 0.15 M octadecylthiol in methanol for at least 4 h, thereby allowing the formation of covalent bonds between the thiol groups and the gold surface and leaving a hydrophobic surface. After incubation, the coated grids were washed with ethanol and dried in a stream of N_2.

The grids were then covered with 2 μL of 4% squalene in hexane on each side before carrying out the deposition [11–13]. Once the hexane had evaporated, a thin film of squalene covered each hole of the dried substrates providing a highly hydrophobic region that stabilized the bilayer formation. The monolayer of the desired lipid composition was first compressed up to 30 mN/m, and then the surface pressure was kept constant and the formation of the PLB proceeded via a LB transfer. The TEM grids were lowered vertically into the lipid monolayer at the

air–water interface and then left submerged overnight. This time is reported to be sufficient to allow equilibration and ensured that the excess squalene trapped between layers of the free standing lipid bilayer diffused out into solution [11,12].

2.4.2. Giant unilamellar vesicles GUVs

Giant unilamellar vesicles (GUVs) were prepared in a homemade Teflon chamber with platinum electrodes, following the electroformation method described by Angelova et al. [14]. Briefly, 3 µL (of a 0.2 mg/mL stock solution) of the lipid mixture in $Cl_3CH:CH_3OH$ containing 1 mol% PE-Rho was spread over the electrodes. After solvent removal in a vacuum chamber, the lipids were hydrated using an aqueous solution of 300 mM sucrose at 50 °C, followed by the application of a sinusoidal wave using the function generator UNI-T UTG9002C (Uni-Trend Group Limited, Hong Kong) with an amplitude of 1.3 V and a frequency of 10 Hz. After the electroformation was carried out for 15 min, a small aliquot of the GUV suspension was transferred to a Lab-Tek coverglass containing an iso-osmotic glucose solution. This coverglass had been previously treated with a 10 mg/mL BSA solution, and thus was covered with a layer of BSA that prevented GUV rupture on the slide, thereby allowing the GUVs to sink to the bottom of the chamber due to the sucrose/glucose density gradient, and facilitating their observation by confocal microscopy (Olympus FV 300, Tokyo, Japan).

The compositions prepared were X_{DPPC} = 0.15, 0.2 and 0.5. The determination of the areas corresponding to each phase was performed in at least 10 images of the polar region of 40 GUV for each composition. The informed values are an average of these determinations at each GUV composition.

2.5. Registration and analysis of the images

The presence or absence of phase coexistence was determined by observing the films with fluorescence microscopy (FM). Images were acquired with confocal microscopy (Olympus FV 300, Tokyo, Japan) in the case of the GUVs and for the rest of the systems with an inverted fluorescence microscope Axiovert 200 (Carl Zeiss, Oberkochen, Germany) equipped with a CCD video camera iXON (Andor, Belfast, Northern Ireland) and a 20× (Zeiss, air immersion, long distance, NA = 0.4) or a 100× (Zeiss, water immersion, NA = 1.0, WD = 1.7 mm) objective. The fluorescent probe was incorporated in the lipid solutions before forming the films (1 mol%), with the concentration of PE-Rho being lower in the liquid condensed (LC) phase than in the liquid expanded (LE) phase. In this way, the LC phase was detected as dark regions in the micrographs.

The distribution coefficient of PE-Rho (D) in LMs, GUVs, SMLs and both kinds of SBLs was determined from FM images for the composition X_{DPPC} = 0.5, using 1 and 0.5 mol% of the fluorescent probe, with the same results being obtained for both concentrations. For the calculation of D, data from images from at least three independent experiments were analyzed (5 images or more) as follows: the gray level inside a domain and in the surrounding LE phase was determined in different regions of the images, with the D value being calculated as the ratio:

$$D = \frac{C_{LC}}{C_{LE}} = \frac{GL_{LC}-DS}{GL_{LE}-DS} \tag{1}$$

where C_{LC} and C_{LE} are the probe concentrations in the LC and the LE phase respectively; GL_{LC} and GL_{LE} are the gray levels in each phase; and DS is the dark signal (gray level in the absence of a fluorescent film, i.e. the background signal). The reported D values are averages of those calculated for different regions of the 5 or more images.

For Eq. (1) to hold, the quantum yield of PE-Rho must be independent of the phase state where it is inserted. Thus, to asses if Eq. (1) can be used for our systems, the gray level of the images taken of monolayers in different phase states and with increasing amounts of PE-Rho was determined. To carry this out, monolayers of a phospholipid in

the LE phase and the same phospholipid with cholesterol (liquid-ordered phase state) were used. Linear plots of the gray level minus the background as a function of the surface concentration of PE-Rho were obtained with slopes of $32 \pm 3 \times 10^2$ nm²/mol% (R^2 = 0.979) for the LE monolayers and $30 \pm 1 \times 10^2$ nm²/mol% (R^2 = 0.996) for the liquid-ordered monolayers (data not shown).

In order to asses if the fluorescent probe had modified the phase behavior of the mixture, the results obtained with FM in monolayers at the air–water interface were compared with the images obtained with Brewster angle microscopy (BAM), where no probe is required. For these experiments, the monolayers under compression were observed using an EP3 Imaging Ellipsometer (Accurion, Goettingen, Germany) with a 20× objective. Since the LE phase was thinner than the LC phase and presented a lower refractive index, it was observed as darker regions in the micrographs [15].

The presence of nano-domains was explored with atomic force microscopy (AFM) using an Innova atomic force microscope (Bruker, Billerica, Massachusetts), with height and phase contrast images being acquired in tapping mode using a silicon probe with a nominal spring constant of 40 N/m and a resonance frequency of 300 kHz. This set of equipment only permits images to be taken in air (dried samples), and thus only SMLs were observed with AFM.

The analysis of the images and the quantification of the area of each phase in coexistence were carried out using Image J software as detailed in Caruso et al. [16].

3. Results and discussion

3.1. Surface pressure-area isotherms and phase diagram

Fig. 1 shows representative compression isotherms for monolayers composed of DPPC, DLPC and their mixtures at the air–water interface at 21 ± 1 °C. The DPPC isotherm showed a typical LE-LC phase transition at π ≈ 4–5 mN/m [17]; while DLPC exhibited the more fluid behavior expected considering that the chain melting phase transition for DLPC is −1 °C [18], which is far below the temperature of these compression isotherms. The collapse pressure obtained under our conditions of compression and temperature was 67 ± 3 mN/m for DPPC and 49 ± 3 mN/m for DLPC. The phase transition in mixed films appeared at higher lateral pressures as the amount of DLPC increased. The variation of the phase transition and the collapse point with the lipid composition suggested that DPPC and DLPC were partially miscible at the air–water interface [19]. For monolayers with X_{DPPC} ≤ 0.5, the DPPC phase transition was
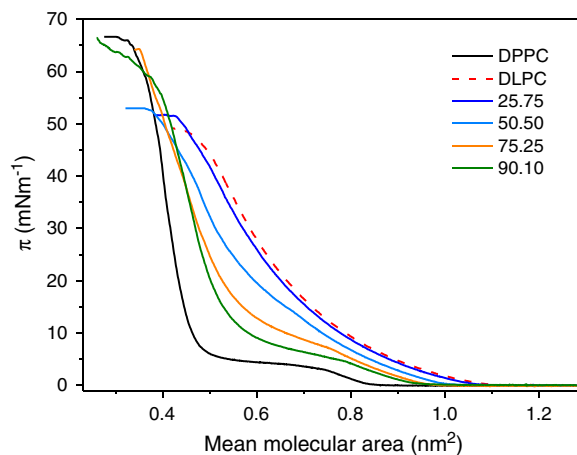

Fig. 1. Representative compression isotherms for monolayers composed of DPPC and DLPC at 21 ± 1 °C.

no longer detectable. All these results are in agreement with those reported by Sanchez et al. [4].

Fig. 2 shows the phase diagram (π vs. X_{DPPC}) constructed using the data taken from the compression isotherms, together with the BAM and FM images for the DPPC/DLPC mixture. The filled and empty circles delimitate the area where two-phase coexistence was observed using BAM or FM, respectively, and these data points coincided with the onset of the phase transition determined from the compression isotherm at DPPC proportions of 50 mol% or higher (dashed line with triangles). As can be observed in Fig. 2, the values obtained from the BAM images showed a good agreement with the data taken from the FM images, indicating that PE-Rho did not affect the phase diagram of monolayers composed of DPPC:DLPC mixtures.

As Langmuir monolayers can be compressed, the surface pressure can be controlled. However, this is not possible in free-standing bilayers or in supported films, and consequently, the comparison between the different membranes was performed at a fixed surface pressure of 30 mN/m, where the monolayers showed phase coexistence in the range $0.17 < X_{DPPC} < 0.99$.

Interestingly, at 30 mN/m three levels of gray were observed in the range $0.75 < X_{DPPC} < 0.85$ (triangles in Fig. 2A), with the third gray level appearing at 20–25 mN/m in the border of the LC domains (see Fig. 2D). Since the presence of three gray levels has not been previously reported for this mixture, experiments with a higher resolution were performed using supported films that led to the conclusion that it was a consequence of low resolution, which precludes the observation of small structures. These results are shown and explained in Section 3.2.1. For $X_{DPPC} \geq 0.85$, the images turned blurry at high surface pressures, and although the domains disappeared to form a homogeneous phase before collapse, an accurate determination of the π value at which phases became indistinguishable was difficult. For this reason, at some points the domain disappearance and appearance was determined by compression and expansion respectively, and a defined limit is not indicated for phase coalescence in this region of the phase diagram.

3.2. Supported membranes

3.2.1. Transferred from monolayers

Supported monolayers and bilayers were generated using a circular hydrophilic coverglass as the substrate. The deposition pressure was 30 mN/m, with both systems being observed by FM using PE-Rho as

the florescent probe. Fig. 3 shows representative images obtained for these systems at 21 ± 1 °C. In the SML films, two phases were observed for $0.40 \leq X_{DPPC} < 0.90$, and for values of X_{DPPC} higher than 0.60, three gray levels appeared, and showed a similar pattern as that in Langmuir monolayers. For both SBL films (^{d}SBLs and ^{p}SBLs), domains were observed between $0.35 \leq X_{DPPC} < 0.9$, with the apparition of the third gray levels at X_{DPPC} higher than 0.7. All the supported films were stable over time, and their textures were unchanged after overnight equilibration.

The observation of a third gray level in a certain range of compositions for Langmuir monolayers and for the supported films transferred from monolayers has not been previously reported for DPPC:DLPC mixtures. Thus, in order to get insight into this phenomenon, the SLMs were observed with higher resolution. Using a 100× objective, thin branches around each domain were observed (see Fig. 4B). These branches appear as gray regions at low resolution (using a 20× objective), as shown in Fig. 4A.

Therefore, the intermediate level of gray observed in Figs. 2D and 4A was an artifact due to thin structures that could not be completely resolved with the resolution of images taken with the 20× objective. These branched domains appear to be formed at the air–water interface and they remained in the solid support. BAM images of Langmuir monolayers in this region of the phase diagram were taken using the minimum compression velocity allowed by the equipment (0.7 Å^2 molecule^{-1} min^{-1}). Once the third gray level appeared, a stepwise compression was performed, waiting 1 min at each surface pressure and thus allowing the monolayer to equilibrate. However, this experiment led to similar monolayer textures as those observed in monolayers compressed at normal rates, and thus it was not possible with our experimental set-up, obtaining less branched domains at these lateral pressures and compositions. The aim of this work was to compare the phase behavior of the different model membrane systems, which can be performed regardless of the film texture. Furthermore, the experiments performed with freshly prepared lipid solutions using different lipid batches and at different compression rates lead to similar results, and thus the texture and phase composition were reproducible in our experimental conditions.

3.2.2. Transferred from SUVs

SUVs were obtained for different DPPC:DLPC mixture compositions ($X_{DPPC} = 0.25, 0.5, 0.75$) with a major population of ~30 nm diameter,

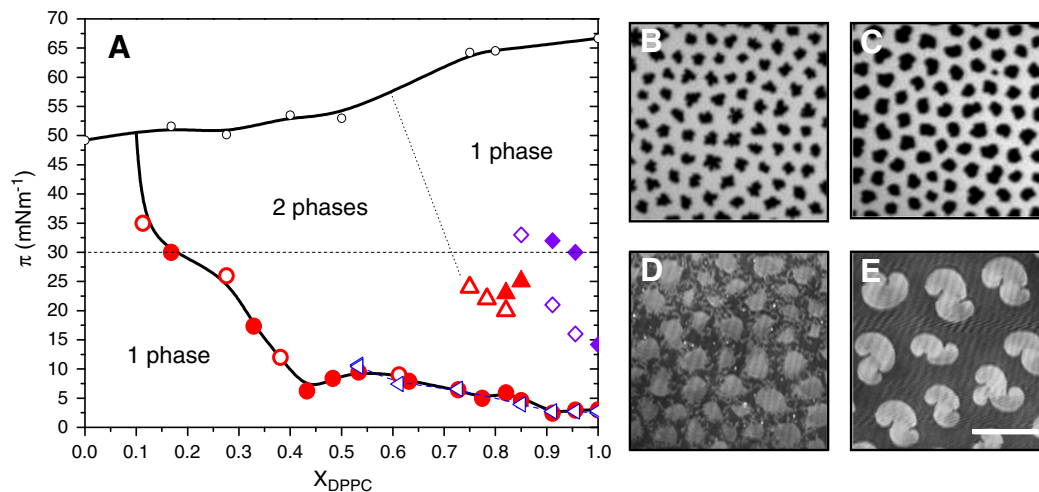**Fig. 2.** (A) Phase diagram (π vs. X_{DPPC}) for monolayers composed of DPPC:DLPC at 21 ± 1 °C. Surface pressure at which domains appeared determined with BAM (●) or FM (○); regions in which three gray levels appeared determined with BAM (▲) or FM (△). Collapse pressure (○), DPPC transition pressure (-◁-) detected from the compression isotherm, and disappearance of domains determined by compression (◆) or expansion (◇). The dashed line indicates the surface pressure at which the different model membranes were compared (π = 30 mN/m). Representative images taken with FM (B and C) or BAM (D and E) at regions of the phase diagram where two phases coexisted: (B) $X_{DPPC} = 0.5$, π = 30 mN/m; (C) $X_{DPPC} = 0.8$, π = 15 mN/m; (D) $X_{DPPC} = 0.8$ (region with three gray levels), π = 30 mN/m, and (E) $X_{DPPC} = 0.95$, π = 4 mN/m. Image sizes: 150 × 150 μm^2, scale bar: 50 μm.

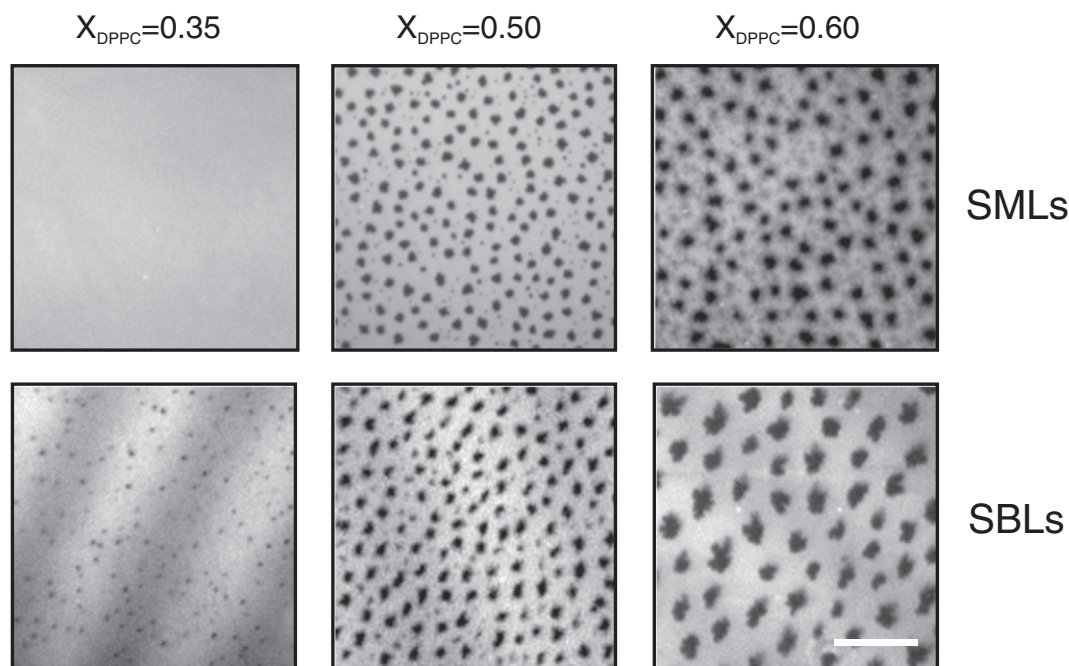**Fig. 3.** Images of the supported membranes, monolayers (SMLs) or bilayers (SBLs) taken with FM using a 20× objective. Image sizes: 168 × 168 μm². The scale bar is 50 μm.

which were then transferred onto hydrophilic circular coverglasses. The images registered with FM showed that the rupture and fusion of the SUVs over the supports were effective, but microscopic domains were not observed.

Multilamellar vesicles composed of this mixture have been previously studied with differential scanning calorimetry, and at 20 °C demixing was observed for X_{DPPC} values in the range 0.25 to 0.80 [18]. Additionally, Ipsen et al. calculated the phase diagram for bilayers of this mixture, and determined the presence of phase coexistence for $0.22 \leq X_{DPPC} \leq 0.81$ at 20 °C [20]. Therefore, the presence of phase coexistence in SUVs was also expected, implying the presence of a population of SUVs in the LE phase and another population in the LC phase; or both phases for each SUV. When 30 nm diameter SUVs fuse to the glass to form supported bilayers, domains of 0.03 μm² or smaller may form, then if there is no reorganization of

the film on the surface, domains remain with sizes of less than a micron. The presence of domains of this size cannot be detected with FM, and a higher resolution technique such as AFM should be used. However, we were not able to perform AFM in samples underwater and therefore, it was not possible to check the presence of nano-domains in this system. Nevertheless, as the observation of nanoscopic domains by AFM were previously reported for DPPC:DLPC bilayers generated by the rupture of large unilamellar vesicles on mica [21], small domains whose size was below the resolution of optical microscopy may have been present also in our experiments.

Some studies have shown domain nucleation to take place when cooling a supported film previously heated to above the transition temperature [22–24]. Hence, we heated the SVRs to check if lipid reorganization could result in the generation of microscopic domains. However,
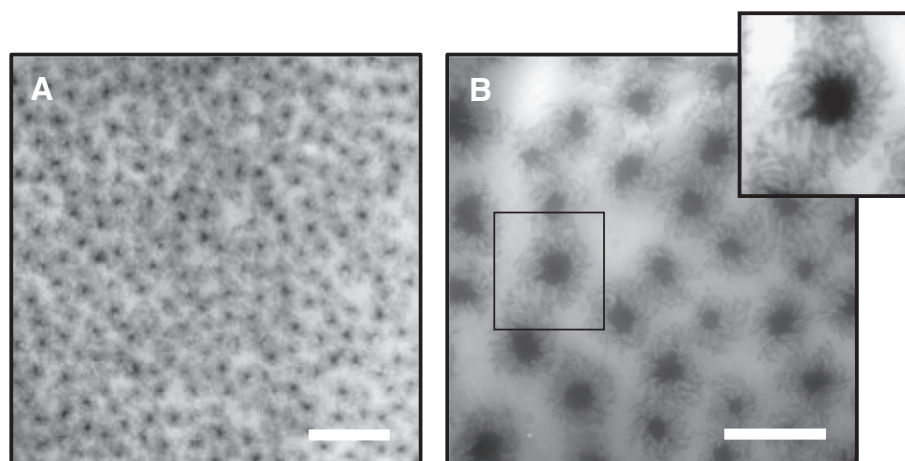

Fig. 4. FM images of SLMs composed of DPPC:DLPC with $X_{DPPC} = 0.6$, using 0.5 mol% PE-Rho. (A) Image taken with a 20× objective, three gray levels are observed. Image size: 250 × 250 μm². Scale bar: 50 μm. (B) Image taken with a 100× objective. The third gray level observed in A corresponded to thin structures below the resolution of image A. Image size: 100 × 100 μm². Scale bar: 25 μm.

after cooling down the samples to room temperature 21 ± 1 °C, no microscopic domains were observed.

3.3. Freestanding lipid bilayers

3.3.1. Planar lipid bilayers

Planar bilayers were generated by transferring monolayers of different DPPC:DLPC compositions to both sides of hydrophobic gold grids at a surface pressure of 30 mN/m. The deposition was performed in a Langmuir balance placed on the stage of the microscope, and thus the texture of the monolayer was controlled before transferring it to the grids, with the transferred bilayer being observed immediately by FM and after an overnight equilibration in order to eliminate the excess squalene. The fluorescence micrographs showed an effective transference for all the tested compositions (X_{DPPC} = 0.35; 0.4; 0.5; 0.7; 0.75; 0.8), but phase coexistence was not observed in any of the samples. This result was unexpected, since phase coexistence was reported for this mixture in GUVs [25], with the only difference being that other fluorescent probes were employed. However, any effect resulting from the probe was discarded (see the following Section).

It has been reported that planar bilayers do not necessary retain the phase behavior of the transferred monolayers. In addition, Hauss et al. [26] demonstrated using neutron diffraction that the squalene lay predominantly between the hemilayers, parallel to the plane of the membrane. Thereby, it is possible that some of the squalene retained in the grids affected the properties of the bilayers and/or that a redistribution of the phases in smaller LC clusters occurred.

3.3.2. GUVs

Fidorra et al. [25] reported a phase diagram for GUVs composed of DPPC:DLPC mixtures together with the quantification of each phase area in the region of the phase diagram with two phases using a very accurate method. Since these authors used different fluorescent probes, in order to use their data and compare their results with ours we first corroborated that the phase boundaries using PE-Rho were similar to those reported in ref. [25]. GUVs composed of DPPC:DLPC and 1 mol% PE-Rho were prepared by the electroformation method and observed by confocal microscopy. The GUV compositions were X_{DPPC} = 0.15, 0.2 and 0.5, and at least forty GUVs of each mixture were registered. For X_{DPPC} = 0.15, 75% of the observed GUVs did not show phase coexistence, while for X_{DPPC} = 0.20 and X_{DPPC} = 0.5, 93% of the observed GUVs presented domains. Therefore, the lower boundary of the phase diagram using PE-Rho lay in the range X_{DPPC} = 0.15–0.20, which is in agreement with data reported by Fidorra et al. (X_{DPPC} = 0.18). It is worth remarking that it was not expected that 100% of the population would show the same behavior due to the fact that the composition in GUVs is known to have a broad distribution (i.e., it varies from one GUV to the other) [27].

The percentage of each phase in coexistence for the GUVs prepared with PE-Rho at compositions X_{DPPC} = 0.2 and 0.5 were similar to those reported by Fidorra et al.: $A^e/A^c = (3 \pm 1)$ for X_{DPPC} = 0.2, and $A^e/A^c = (0.5 \pm 0.2)$ for X_{DPPC} = 0.5 (see next Section). Taking into account these controls, it can be assumed that PE-Rho did not affect the phase behavior of these GUVs and that the results published by Fidorra et al. may be used in order to compare them with the results found in this work.

3.3.3. Comparison of the model membrane systems

It is not possible to control the molecular area as in the case of monolayers, either in supported membranes or in freestanding bilayers. So that the properties of each system could be analyzed and compared, a pressure of 30 mN/m was selected, since it has been previously postulated that between 30 and 35 mN/m the mean molecular area in bilayers is equivalent to that observed in monolayers [8,9]. However, we are aware that it has also been reported that thermal fluctuations in bilayers may lead to variations in the lateral pressure of at least 15 mN/m [10].

A summary of the compositions of the phase boundaries of the analyzed model membranes found in the present study is shown in Table 1, along with the reported values.

In order to make a thermodynamic comparison between the different systems, the total area occupied by each phase was calculated for all DPPC:DLPC compositions of each model membrane. The regions in which three gray levels were observed using the 20× objective were excluded in the analysis, since the quantification of the coexisting areas were not so reliable in those regions of the phase diagram. Thus, only the data obtained for DPPC molar fractions lower than those where three gray levels were observed in each system are shown.

Fig. 5a shows a comparison of the area ratios A^e/A^c (area of the LE phase divided by the area of the LC phase) versus the molar fraction of DPPC for the studied systems that presented micron-sized domains. These ratios should follow the lever rule, i.e. their values depend on the compositions of the coexisting phases, and thus the differences between sets of data depicted in Fig. 5a imply different phase diagrams [16,25].

The values obtained for LMs were only slightly higher than the GUV ratios [25] (see Fig. 5A). On comparing the data published for GUVs with data of monolayers for surface pressures between 20 and 40 mN/m, it was found that the area ratios of the LMs were always slightly higher than the GUV ratios at these surface pressures, and thus the slight difference was not related with the chosen surface pressure.

Fig. 5A also shows that in contrast with GUVs and LMs, the supported systems presented a different trend, with the amount of the LC phase at some X_{DPPC} being lower for ^{d}SBLs and SMLs compared to the freestanding films (GUVs and LMs). Hence, in the supported films, either the number of domains was lower (some domains disappeared when the monolayer was transferred), or the domains themselves were smaller. Fig. 5B shows the average size of the domains (average domain area) and the number of domains per unit of area (domain density) for LMs, ^{d}SBLs and SMLs as a function of the mole fraction of DPPC, and it can be observed that while the domain density was similar for all the analyzed systems, the domains were larger in monolayers than in supported membranes (i.e. domains were reduced in size when the monolayer was transferred to the glass).

As mentioned above, nano-domains have been observed in supported membranes transferred from vesicles [21], as well as in DPPC/DLPC monolayers transferred onto $C_{14}SH$-Au modified substrates by the Langmuir–Schaefer technique [4]. These reported observations, together with the decrease in the size of the micro-domains shown in Fig. 5B, suggest a possible reorganization of the phases with formation of nano-domains (coexisting with the micro-domains) that we might not have been able to quantify due to the limited resolution of FM. In order to investigate this possibility we searched for SLMs using AFM. As explained before, the AFM equipment used in this work only allowed determining the topography of surfaces in air, and not in an aqueous solution. SLMs films are stable in air, while SBLs and SVRs have to remain in the aqueous solution, since if they dry, a rearrangement would occur and therefore, only SLMs were observed with AFM.

Fig. 6 shows a representative image of the topography of SMLs determined with AFM showing that nano-domains were not observed in these films, and thus, the differences in the area ratios shown in Fig. 5

Table 1
Summary of the phase boundaries of the analyzed systems.

	LMs	SMLs	SBLs	SVRs	GUVs
X^e	0.17[a]	0.4[a]	0.35 [a]	0.46 [b]	>0.15 and <0.20[a] 0.28[b]–0.18[c]
X^c	0.95[a]	0.9 [a]	0.9 [a]	0.89 [b]	0.87[b]–0.84[c]

DPPC molar fraction in the expanded phase (X^e), and DPPC molar fraction in the condensed phase (X^c). [a]Data obtained in this work or data taken from [b]Tokumasu et al. [21] and [c]Fidorra et al. [25].
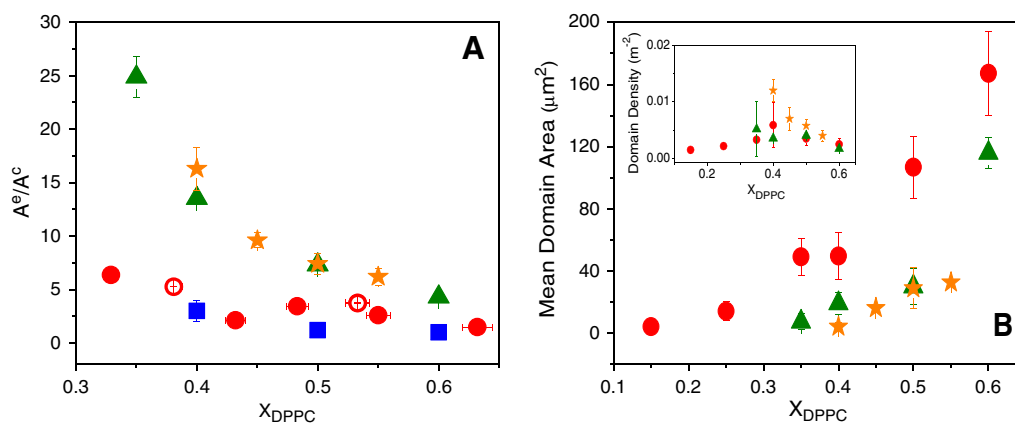
Fig. 5. (A) Area ratios of the phases A^e/A^c vs. DPPC molar fraction for the different systems with micron-sized domains. GUV data taken with permission from [25]; (B) Mean Domain Area (μm^2) vs. DPPC molar fraction. Inset: Domain Density (μm^{-2}) vs. DPPC molar fraction. Symbols: LM using BAM (●) or FM (○); GUVs (■); ^{d}SBLs (▲); SMLs (★).

derived from a difference in the composition of the coexisting phases and not from a rearrangement of the domains.

As already indicated, it has been reported that the presence of nano-domains in SVRs of this mixture on mica [21], and thus they may be present in the SVRs showed here. In the case of SBLs on glass, to the best of our knowledge, AFM images have not been reported for this mixture, and since the FM images of SBLs and SMLs were similar, it may be assumed that nano-domains were not present in the SBLs that are shown in this work, indicating that the compositions of the coexisting phases in SBLs and SMLs were similar and different to those found in GUVs and LMs.

The same area ratio was obtained for SMLs using FM as that using AFM, with Table 2 showing the values at $X_{DPPC} = 0.5$ for both techniques. This table also shows the area ratio for the SBL films, and it can be observed that the average area ratio for ^{d}SBLs was similar to that for ^{p}SBLs, i.e. the composition of the phases was the same regardless of the order in which the monolayers were transferred. This result rules out any effects that may have arisen as a consequence of flip-flop between the leaflets, as previously observed in other supported films [6]. In addition, it suggests that short range interactions between the proximal leaflet and the glass did not influence noticeably the phase diagram of the transferred film. Therefore, the differences observed between the free-standing and supported films, which indicate that the support affected the membrane phase behavior, may have been related to a loss of degrees of freedom in the supported films. In this

regard, similar effects derived from entropy suppression have been reported for DPPC/DLPC/cholesterol films on mica [21], and even the absence of the ripple phase in supported bilayers has been previously observed [28].

Another important observation suggested by our results is that inter-leaflet interactions did not markedly alter the phase diagram of the films, since on one hand, the GUVs were comparable with the LMs and on the other hand, there were only slight differences observed between the SLMs and SBLs.

Comparing the images of LMs, SMLs and SBLs (e.g. images shown in Fig. 2B, and C compared with those in Fig. 4 for $X_{DPPC} = 0.5$), it can be observed that the gray levels were not the same in each type of model membrane, indicating that the concentration of PE-Rho in each phase changed from one system to the other. Therefore, we calculated the fluorescent probe distribution coefficient (D), as described in Section 2.5 for images with $X_{DPPC} = 0.5$ and with 0.5 and 1 mol% of PE-Rho. The value of D obtained was the same (within errors) at both probe concentrations in each system, with the average being shown in Fig. 7, where it can be observed that D increased in the order GUVs < LMs < ^{p}SBLs ≃ ^{d}SBLs < SMLs.

A different D value would imply that the properties that the probe senses are not the same within the systems (probably the density, the stiffness and/or other order parameter of the phases are changing). As a value of $D = 1$ implies no preference of the probe for the coexisting phases, then as D approaches unity, the coexisting phases became
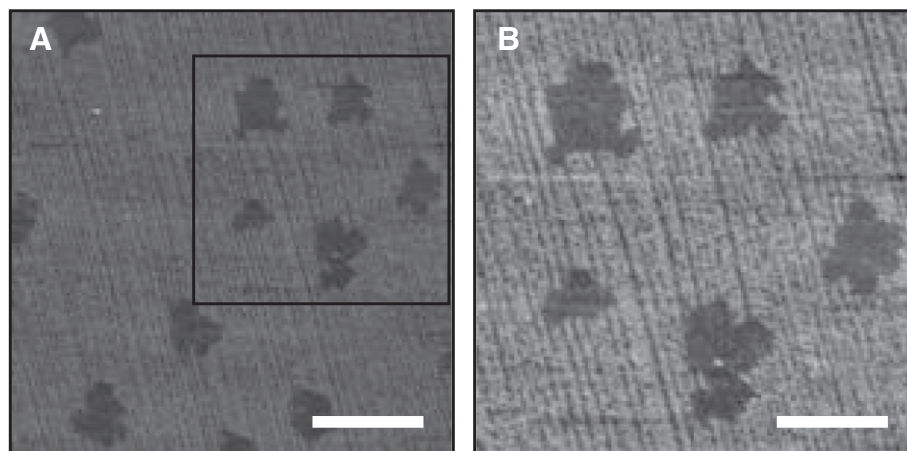

Fig. 6. AFM phase images of SML of DPPC:DLPC 50:50 composition. (A) Image size is $20 \times 20 \ \mu m^2$ and the scale bar is 5 μm. (B) Higher magnification image ($12 \times 12 \ \mu m^2$) of the region indicated with a square in (A). The scale bar is 3 μm.

Table 2
Area ratios for supported systems $X_{DPPC} = 0.5$.

System	Ae/Ac
SMLs	7 ± 1 (FM)
	9 ± 1 (AFM)
^{d}SBLs	7.3 ± 0.4 (FM)
^{p}SBLs	7.4 ± 0.8 (FM)

Area ratios of LE and LC phases measured by FM and AFM.

more similar, and thus the LE phase turned into a more condensed-like phase and/or the LC phase was more expanded.

The composition of the coexisting phases in the supported films was different to that in GUVs and LMs. As shown in Table 1, in the supported films the expanded phase was enriched in DPPC ($X_{DPPC} \sim 0.2$ for LMs and GUVs and $X_{DPPC} \sim 0.4$ for the supported films), which could be related with an increment in the order of the hydrocarbon chains, and consequently the properties of the expanded phase would be more similar than those of the condensed phase. However, GUVs and LMs showed similar phase boundaries and thus, the marked differences observed in the D value were related to a change in the phase properties not derived from a change in their compositions.

4. Conclusions

In this study we have analyzed the phase diagram of films composed of DPPC and DLPC using different model membranes with the aim of comparing their thermodynamic properties. Our results show that the compositions of the coexisting phases at 21 ± 1 °C in LMs and GUVs were only slightly different, while in supported membranes the borders of the phase diagrams were shifted to higher DPPC proportions, and thus the expanded phase in SMLs and SBLs was enriched in DPPC (slightly higher for SMLs than for SBLs, see Table 1). The differences observed in the compositions of the coexisting phases between free-standing and supported films were not due to short-distance specific interactions between the glass and the lipid membrane, since a similar result was found when the analyzed hemilayer was the distal leaflet or the proximal leaflet. Thereby, we suggest that the differences present in supported compared to free-standing films were a consequence of a suppression of entropy due to the presence of the rigid support, as previously observed for films on mica [21].

Both the phase diagram and the distribution of the fluorescent probe indicate that the properties of the expanded and the condensed phases were more similar in supported films than in free-standing films,
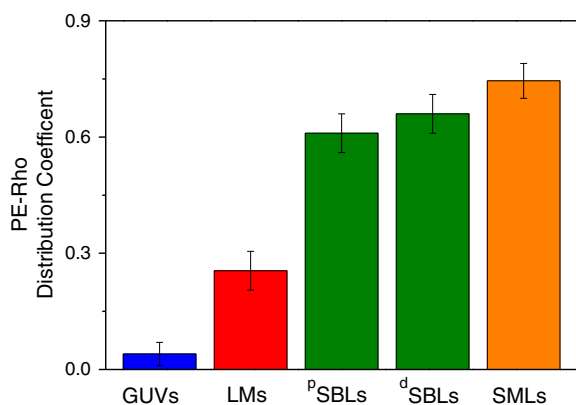
probably due to the expanded phase becoming more rigid and thus more condensed-like as a result of the proximity to the rigid support. Related to this, it has been previously reported that the ripple phase in supported bilayers is suppressed, thereby changing the phase properties of the film [28].

Bilayers formed on a hollow grid, as well as on glass from the rupture of vesicles did not show any micron-sized domains. However, with the technique used (fluorescence microscopy), it was not possible to discard the presence of two-phases with an LC phase arranged in nano-domains. Assuming that two-phases were also present in these systems, it can be concluded that the texture of the film (the distribution of the coexisting phases in the plane of the membrane) depends on the model system.

Only slight differences were found in the phase boundaries of monolayers compared to bilayers (LMs with GUVs and SLMs with SLBs), indicating that inter-leaflet interactions did not markedly affect the phase diagram of this mixture. The trend observed in the distribution coefficient of PE-Rho was: GUVs < LMs < ^{p}SBLs $\simeq$ ^{d}SBLs < SMLs. This correlated with the degrees of freedom of the systems: in GUVs, the membrane can fluctuate out-of-plane freely, whereas in LMs this motion is restricted, and in supported films it is precluded due to the rigid support. This suggests that the loss in entropy promotes LC and LE phases that were more similar in the order: GUVs < LMs < ^{p}SBLs $\simeq$ ^{d}SBLs $\simeq$ SMLs, and thus the fluorescent probe preferring the LE phase over the LC phase, but in a less marked fashion.

It is very important to understand the limitations of each experimental model in order to determinate the validity of the measured parameters, and in which manner the general trends observed in a given model can be extended to other models and to cellular membranes. Here, we have made a comparison between free-standing and supported films prepared in different ways and found comparable general features in some of the model systems. However, a more quantitative analysis led us to conclude that the properties of the coexisting phases were not the same within the systems. Indeed, even in a simple binary mixture of phospholipids that did not show a strong specific interaction with the support, the properties of the phases are not quantitatively equal along the different model membranes. Therefore, in a more complex system such as biological membranes, the interaction with cytoskeletal proteins, neighboring membrane stacks, and extracellular matrices, most likely affects the properties of native lipid phase behavior.

Fig. 7. Average distribution coefficients (D) of the fluorescent probe PE-Rho in all the analyzed systems that showed micron-sized domains. The errors correspond to the standard deviation of the determined individual D values (see Section 2.5) and are similar to the differences between values at 0.5 and 1 mol% of PE-Rho.

References

[1] A.C. Simonsen, L.A. Bagatolli, Structure of spin-coated lipid films and domain formation in supported membranes formed by hydration, Langmuir 20 (2004) 9720–9728.

[2] W.C. Lin, C.D. Blanchette, T.V. Ratto, M.L. Longo, Lipid asymmetry in DLPC/DSPC-supported lipid bilayers: a combined AFM and fluorescence microscopy study, Biophys. J. 90 (2006) 228–237.

[3] M. Seul, M.J. Sammon, Preparation of surfactant multilayer films on solid substrates by deposition from organic solution, Thin Solid Films 185 (1990) 287–305.

[4] J. Sanchez, A. Badia, Atomic force microscopy studies of lateral phase separation in mixed monolayer of dipalmitoylphosphatidylcholine and dilauroylphosphatodylcholine, Thin Solid Films 440 (2003) 223–239.

[5] G. Pabst, N. Kucerka, P. Nieh, M.C. Rheinstadter, J. Katsaras, Applications of neutron and X-ray scattering to the study of biologically relevant model membranes, Chem. Phys. Lipids 163 (2010) 460–479.

[6] H.P. Wacklin, Composition and asymmetry in supported membranes formed by vesicle fusion, Langmuir 27 (2011) 7698–7707.

[7] R.P. Richter, A.R. Brisson, Following the formation of supported lipid bilayers on mica: a study combining AFM, QCM-D, and ellipsometry, Biophys. J. 88 (2005) 3422–3433.

[8] R.A. Demel, W.S. Geurts van Kessel, R.F. Zwaal, B. Roelofsen, L.L. van Deenen, Relation between various phospholipase actions on human red cell membranes and the interfacial phospholipid pressure in monolayers, Biochim. Biophys. Acta 406 (1975) 97–107.

[9] D. Marsh, Lateral pressure in membranes, Biochim. Biophys. Acta 1286 (1996) 183–223.

[10] M.C. Phillips, D.E. Graham, H. Hauser, Lateral compressibility and penetration into phospholipid monolayers and bilayer membranes, Nature 254 (1975) 154–156.

[11] C.W. Harland, M.J. Bradley, R. Parthasarathy, Phospholipid bilayers are viscoelastic, Proc. Natl. Acad. Sci. U. S. A. 107 (2010) 19146–19150.

[12] M.D. Collins, S.L. Keller, Tuning lipid mixtures to induce or suppress domain formation across leaflets of unsupported asymmetric bilayers, Proc. Natl. Acad. Sci. U. S. A. 105 (2008) 124–128.

[13] S.H. White, Formation of "solvent-free" black lipid bilayer membranes from glyceryl monooleate dispersed in squalene, Biophys. J. 23 (1978) 337–347.

[14] A. Angelova, S. Soleau, Ph. Meleard, F. Faucon, P. Bothorel, Preparation of giant vesicles by external AC electric fields. Kinetics and applications, Prog. Colloid Polym. Sci. 89 (1992) 127–131.

[15] F. Vega Mercado, B. Maggio, N. Wilke, Phase diagram of mixed monolayers of stearic acid and dimyristoylphosphatidylcholine. Effect of the acid ionization, Chem. Phys. Lipids 164 (2011) 386–392.

[16] B. Caruso, A. Mangiarotti, N. Wilke, Stiffness of lipid monolayers with phase coexistence, Langmuir 29 (2013) 10807–10816.

[17] H. Mohwald, Phospholipids monolayers, in: R. Lipowsky, E. Sackmann (Eds.), Structure and Dynamics of Membranes, Elsevier, Amsterdam, 1995, pp. 161–211.

[18] P.W.M. VanDijk, A.J. Kaper, H.A.J. Oonk, J. De Gier, Miscibility properties of binary phosphatidylcholine mixtures, Biochim. Biophys. Acta 470 (1977) 58–69.

[19] G.L. Gaines, Insoluble Monolayers at Liquid–gas Interfaces, Interscience Publishers, New York, 1966.

[20] J.H. Ipsen, G. Karlstrom, O.G. Mouritsen, H. Wennerstrom, M.J. Zuckermann, Phase equilibria in the phosphatidylcholine–cholesterol system, Biochim. Biophys. Acta 905 (1987) 162–172.

[21] F. Tokumasu, A.J. Jin, G.W. Feigenson, J.A. Dvorak, Nanoscopic lipid domain dynamics revealed by atomic force microscopy, Biophys. J. 84 (2003) 2609–2618.

[22] C.D. Blanchette, W.C. Lin, C.A. Orme, T.V. Ratto, M.L. Longo, Domain nucleation rates and interfacial line tensions in supported bilayers of ternary mixtures containing galactosylceramide, Biophys. J. 94 (2008) 2691–2697.

[23] A.J. Garcia-Saez, S. Chiantia, P. Schwille, Effect of line tension on the lateral organization of lipid membranes, J. Biol. Chem. 282 (2007) 33537–33544.

[24] K. Iimura, T. Shiraku, T. Kato, Micro-phase separation in binary mixed langmuir monolayers of n-alkyl fatty acids and a perfluoropolyether derivative, Langmuir 2002 (2002) 10183–10190.

[25] M. Fidorra, A. Garcia, J.H. Ipsen, S. Hartel, L.A. Bagatolli, Lipid domains in giant unilamellar vesicles and their correspondence with equilibrium thermodynamic phases: a quantitative fluorescence microscopy imaging approach, Biochim. Biophys. Acta 1788 (2009) 2142–2149.

[26] T. Hauss, S. Dante, N.A. Dencher, T.H. Haines, Squalane is in the midplane of the lipid bilayer: implications for its function as a proton permeability barrier, Biochim. Biophys. Acta 1556 (2002) 149–154.

[27] J. Larsen, N.S. Hatzakis, D. Stamou, Observation of inhomogeneity in the lipid composition of individual nanoscale liposomes, J. Am. Chem. Soc. 133 (2011) 10685–10687.

[28] C. Leidy, T. Kaasgaard, J.H. Crowe, O.G. Mouritsen, K. Jorgensen, Ripples and the formation of anisotropic lipid domains: imaging two-component supported double bilayers by atomic force microscopy, Biophys. J. 83 (2002) 2625–2633.